

Natural convection in a right-angle corner : higher-order analysis

D. B. INGHAM

Department of Applied Mathematical Studies, The University of Leeds, Leeds,
West Yorkshire LS2 9JT, U.K.

and

I. POP

Faculty of Mathematics, The University of Cluj, R-3400, Cluj, CP 253, Romania

(Received 6 May 1988 and in final form 16 March 1989)

Abstract—Higher-order boundary-layer effects for natural convection flow in a right-angle corner formed by a semi-infinite vertical plate, which is prescribed with a uniform heat flux, and a semi-infinite horizontal plate, which is thermally insulated, is presented. Using the method of asymptotic matched expansions the solution is obtained up to the fourth-order expansion. For the first time the interplay between the two boundary-layer flows, which takes place through the outer inviscid region, has been investigated. Eigenvalues and their corresponding eigenfunctions which are associated with the inner expansions have been sought and it has been found that their contribution up to fourth-order correction is identically zero. Numerical results have been obtained for Prandtl numbers of 0.72 (air), 1 and 6.7 (water) and the flow in the outer region and the velocity and temperature profiles in the boundary layers are presented. Also the variation of the local Nusselt number and skin friction coefficients on the plates are presented as functions of the local Grashof numbers. It is found that the presence of the horizontal plate has quite a substantial effect on the higher-order approximations in the vertical boundary layer and the outer region.

1. INTRODUCTION

ONE OF the most active areas of research in theoretical convection heat transfer is to determine higher-order boundary-layer approximations in a viscous incompressible fluid for some flow configurations. Previous investigations of natural convection at finite Grashof numbers consists notably of refs. [1–14] for vertical, horizontal and inclined flat plates. Higher-order approximations for the problem of free and mixed convection flow arising from a wall plume and a horizontal line thermal source of heat have also been obtained in refs. [15–19]. For other geometries we may refer to refs. [20, 21]. On the other hand, recent interest in the flow through a porous medium has led to a large number of papers dealing with higher-order effects for the Darcian free and mixed convection boundary-layer flow adjacent to a solid surface that is embedded in a fluid-saturated porous medium. Comprehensive reviews of the literature in this area have recently been made in refs. [22, 23].

The approach used in all these contributions is based on the method of matched asymptotic expansions as described by Van Dyke [24] and Martynenko *et al.* [25]. This concept, which has been successfully applied to a wide variety of singular-perturbation problems in fluid mechanics, prescribes a precise matching scheme in order to completely specify the boundary-layer motion to any desired order.

The problem of higher-order buoyancy-induced

fluid effects in a corner has received relatively little attention. The first analytical approach to this problem, which uses matched asymptotic expansions, is that of Riley and Poots [26] who analysed natural convection flow due to a heated right-angle corner formed by the intersection of two semi-infinite vertical plates. More recently, several authors [25, 27–29] have showed interest in the problem of natural convection in a corner that is formed by a vertical, heated plate which intersects at an arbitrary angle with another unheated plate. Luchini *et al.* [28, 29] formulated this problem using the method of matched asymptotic expansions in combination with a finite difference numerical scheme. The first-order correction to the classical boundary-layer natural convection near a vertical semi-infinite flat plate was extended to find the first-order boundary layer that develops on the inclined plate—the secondary boundary layer. However, the results in refs. [28, 29] do not refer to the effect of the secondary boundary layer on the vertical boundary layer and no discussion of the eigenvalues, and the corresponding eigenfunctions, appear in the boundary-layer expansions.

More recently, Ruiz and Sparrow [30] have performed experiments for the free convection flow in two types of corners, called V- and L-shaped corners, whilst Kim and Kim [31] reported analytical and numerical solutions for the flow along a vertical rectangular corner for Prandtl numbers of 0.72 and 7.0 and the present authors have studied the convective

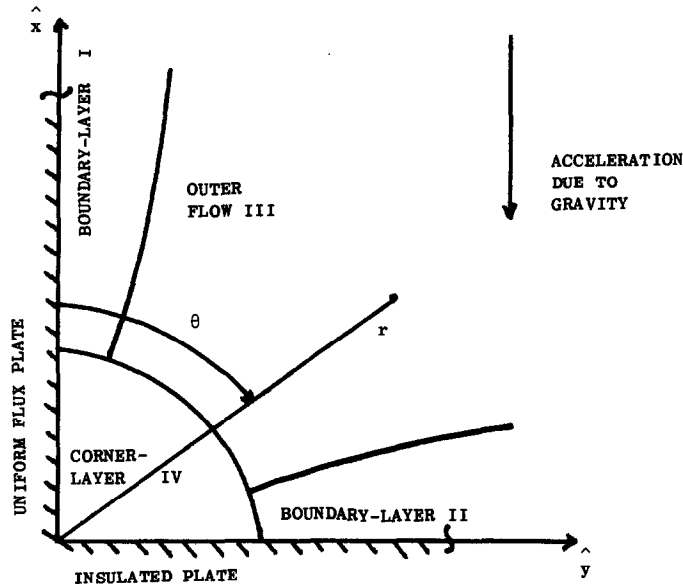


FIG. 1. Corner flow configuration and coordinate system.

for the outflow region III. This procedure may then proceed to further higher-order terms. Both analytical and numerical solutions up to fourth-order terms have been obtained and the flow and temperature functions are presented graphically. The local heat transfer and coefficients of skin friction have been calculated for various Prandtl numbers and results are presented for $\sigma = 0.72$, which corresponds to air, and $\sigma = 1$ and 6.7 , which corresponds to water.

2. GOVERNING EQUATIONS

The mathematical formulation of the problem assumes a steady, viscous and incompressible fluid which obeys the Boussinesq approximation. We assume that the vertical plate is uniformly heated to a constant thermal gradient q , the horizontal plate is insulated and the ambient temperature is T_0 . The vorticity transport and energy equations in non-dimensional form can be written as

$$\left(\frac{\partial \psi}{\partial y} \frac{\partial}{\partial x} - \frac{\partial \psi}{\partial x} \frac{\partial}{\partial y} \right) \nabla^2 \psi = Gr^{-2/5} \nabla^4 \psi + Gr^{1/5} \frac{\partial \Phi}{\partial y} \quad (1)$$

$$\left(\frac{\partial \psi}{\partial y} \frac{\partial}{\partial x} - \frac{\partial \psi}{\partial x} \frac{\partial}{\partial y} \right) \Phi = Gr^{-2/5} \sigma^{-1} \nabla^2 \Phi \quad (2)$$

see, e.g. Afzal [17]. The simplification consequent on the use of these equations is the absence of the pressure from equation (1).

In terms of the usual polar coordinates (r, θ) defined by

$$x = r \cos \theta, \quad y = r \sin \theta \quad (3)$$

equations (1) and (2) are to be solved subject to the following boundary conditions:

$$\psi = \frac{\partial \psi}{\partial \theta} = 0, \quad \frac{1}{r} \frac{\partial \Phi}{\partial \theta} = -1 \quad \text{on } \theta = 0, \quad 0 < r < \infty \quad (4)$$

$$\psi = \frac{\partial \psi}{\partial r} = \frac{\partial \Phi}{\partial \theta} = 0 \quad \text{on } \theta = \pi/2, \quad 0 < r < \infty \quad (5)$$

$$\psi = 0(r), \quad \Phi \rightarrow 0 \quad \text{as } r \rightarrow \infty, \quad 0 < \theta < \pi/2. \quad (6)$$

In the above equations x and y are the (non-dimensional) coordinates measuring distances from the leading edge along the vertical and horizontal plates; ψ the stream function defined such that $(u, v) = (\partial \psi / \partial y, -\partial \psi / \partial x)$; Φ the dimensionless temperature; σ the Prandtl number and ∇^2 denotes the two-dimensional Laplacian. The non-dimensional quantities x, y, ψ and Φ are related to their dimensional counterparts $\hat{x}, \hat{y}, \hat{\psi}$ and \hat{T} by $\hat{x} = xL, \hat{y} = yL, \hat{\psi} = \nu Gr^{2/5} \psi$ and $\hat{T} - T_0 = (qL/k)\Phi$, where $Gr = g\beta qL^4/(k\nu^2)$ is the Grashof number.

3. ANALYSIS

The asymptotic solution of the problem formulated in Section 2 is studied for moderately large values of Gr in the inner boundary-layer regions close to the plates and in the outer region far from the plates. Separate, locally valid expansions for the stream function and temperature in these regions are developed. The outer region is defined for x and y fixed as $Gr \rightarrow \infty$ and the flow can be studied by assuming that ψ possesses in this region an asymptotic expansion of the form

$$\psi = Gr^{-1/5} [\tilde{\psi}_1(x, y) + \delta_2(Gr) \tilde{\psi}_2(x, y) + \delta_3(Gr) \tilde{\psi}_3(x, y) + \text{h.o.t.}] \quad (7)$$

and

$$\Phi \text{ is exponentially small} \quad (8)$$

where the first-order term in expansion (7) is $\tilde{\psi}_0(x, y) \equiv 0$. In later matching requirements the gauge functions $\delta_2(Gr)$ and $\delta_3(Gr)$ will be found to be as given in equations (33) and (48)

$$\delta_2(Gr) = Gr^{-1/10}, \quad \delta_3(Gr) = Gr^{-1/5}. \quad (9)$$

Substitution from expansion (7) into equation (1) and equating terms of the same order of magnitude in Gr gives the equations for $\tilde{\psi}_n$, namely

$$\nabla^2 \tilde{\psi}_n = 0, \quad n = 1, 2, 3. \quad (10)$$

Therefore, to fourth order at least, expansion (7) is valid and the outer flow remains isothermal and irrotational, being governed by the Laplace equation (10).

We now propose to solve the problem systematically by putting together the inner and outer asymptotic expansions.

3.1. First-order boundary layer in region I

Directing attention to the region adjacent to the vertical plate, we take an asymptotic expansion for the stream function ψ and the temperature Φ of the form

$$\psi = Gr^{-1/5}[\psi_0(x, Y) + Gr^{-1/5}\psi_1(x, Y) + \Delta_2(Gr)\psi_2(x, Y) + \Delta_3(Gr)\psi_3(x, Y) + \text{h.o.t.}] \quad (11)$$

$$\Phi = Gr^{-1/5}[\Phi_0(x, Y) + Gr^{-1/5}\Phi_1(x, Y) + \Delta_2(Gr)\Phi_2(x, Y) + \Delta_3(Gr)\Phi_3(x, Y) + \text{h.o.t.}] \quad (12)$$

in which $x(>0)$ and the inner variable $Y(=Gr^{1/5}y)$ are fixed as $Gr \rightarrow \infty$; the gauge functions $\Delta_2(Gr)$ and $\Delta_3(Gr)$ are determined as in equations (36) and (51).

The equations for the leading terms ψ_0 and Φ_0 are obtained by substituting equations (11) and (12) into equations (1) and (2) and retaining the lowest-order terms only. The vorticity equation is then integrated once with respect to the variable Y and the resulting arbitrary function of x set equal to zero due to the matching condition with the first-order outer solution $\tilde{\psi}_0(x, y) \equiv 0$. The resulting equations then permit a similarity solution of the form

$$\left. \begin{aligned} \psi_0 &= x^{4/5}f_0(\eta), \quad \Phi_0 = x^{1/5}h_0(\eta) \\ \text{where} \quad \eta &= Y/x^{1/5} \end{aligned} \right\} \quad (13)$$

and f_0 and h_0 are obtained from

$$f_0''' + \frac{4}{5}f_0f_0'' - \frac{3}{5}f_0'^2 + h_0 = 0 \quad (14)$$

$$\sigma^{-1}h_0'' + \frac{4}{5}f_0h_0' - \frac{1}{5}f_0'h_0 = 0 \quad (15)$$

with the boundary conditions

$$f_0(0) = f_0'(0) = h_0'(0) + 1 = f_0'(\infty) = h_0(\infty) = 0. \quad (16)$$

Here primes denote differentiation with respect to η . These equations are the usual boundary-layer equations for free convection along an unbounded vertical semi-infinite flat plate with a uniform wall flux and the solution can be found in refs. [10, 11].

In order to find further inner term solutions we must match the inner and outer expansions, so we proceed to determine a number of terms of both the inner and outer expansions. The analytical process of matching may be defined in a number of ways, but most appropriate is to use it as described by equation (5.24) from Van Dyke's book [24], namely: "The m -term inner expansion of the (n -term outer expansion) = the n -term outer expansion of the (m -term inner expansion) for any pair of integers m, n ."

3.2. Second-order outer flow in region III

Let us first focus attention on the outer flow and determine the boundary conditions for $\tilde{\psi}_1$. Using the above matching principle, along with the physical boundary condition from equation (5), we obtain

$$\left. \begin{aligned} \tilde{\psi}_1(r, 0) &= r^{4/5}f_0(\infty) \\ \tilde{\psi}_1(r, \pi/2) &= 0. \end{aligned} \right\} \quad (17)$$

Thus, the solution of equation (10) for $\tilde{\psi}_1$ subject to conditions (17) is

$$\tilde{\psi}_1 = -f_0(\infty)r^{4/5} \frac{\sin[\frac{1}{5}(\theta - \pi/2)]}{\sin[\frac{3}{5}\pi]}. \quad (18)$$

3.3. Second-order boundary layer in region I

The matching requirement between the inner and outer longitudinal velocities now demands that the second-order term in equation (11) satisfies

$$\frac{\partial \psi_1}{\partial Y}(x, \infty) = -\frac{4}{5}f_0(\infty) \cot(2\pi/5)x^{-1/5}. \quad (19)$$

We note from equation (19) that all second-order outer streamlines enter the boundary layer I at an angle $2\pi/5$ to the x -axis.

If we now introduce expansions (11) and (12) into equations (1) and (2) and proceed as before we derive equations for ψ_1 and Φ_1 . In these equations we write

$$\psi_1 = f_1(\eta), \quad \Phi_1 = x^{-1/5}h_1(\eta) \quad (20)$$

so that f_1 and h_1 satisfy

$$f_1''' + \frac{4}{5}f_0f_1'' - \frac{3}{5}f_0'f_1' + h_1 = 0 \quad (21)$$

$$\sigma^{-1}h_1'' + \frac{4}{5}f_0h_1' + \frac{3}{5}f_0'h_1 = \frac{1}{5}h_0f_1' \quad (22)$$

together with boundary conditions

$$\left. \begin{aligned} f_1(0) &= f_1'(0) = h_1'(0) = h_1(\infty) = 0 \\ f_1 &\sim -\frac{4}{5}f_0(\infty) \cot(2\pi/5)\eta + A_1, \quad \eta \text{ large} \end{aligned} \right\} \quad (23)$$

where A_1 is an unknown constant. Again, these equations are identical to those for a uniform flux vertical plate in an unbounded region but boundary conditions (23) are different.

3.4. Second-order boundary layer in region II

Since the outer solution (18) does not satisfy boundary conditions (5), a boundary layer develops on the horizontal plate. However, no thermal behaviour exists on this plate since no thermal energy is transmitted to outer region III from the thermal boundary layer in region I. This result is true for all higher-order boundary-layer approximations of the inner region II.

Let the thickness of the boundary layer in region II be $\bar{\Delta}_1(Gr)$ and it is such that it vanishes as Gr increases. The appropriate stretching of the inner normal coordinate X to this plate is then

$$X = x/\bar{\Delta}_1(Gr). \quad (24)$$

Now, from equations (5), (7) and (24) we find that

$$\psi = O(Gr^{-1/5} \bar{\Delta}_1(Gr)) \quad (25)$$

and therefore we assume the following expansion for the inner stream function of region II

$$\psi = Gr^{-1/5} [\bar{\Delta}_1(Gr) \bar{\psi}_1(X, y) + \bar{\Delta}_2(Gr) \bar{\psi}_2(X, y) + \bar{\Delta}_3(Gr) \bar{\psi}_3(X, y) + \text{h.o.t.}] \quad (26)$$

where the gauge functions $\bar{\Delta}_1(Gr)$, $\bar{\Delta}_2(Gr)$ and $\bar{\Delta}_3(Gr)$ are found to be as given in equations (27), (42) and (56). The matching condition is now that the y velocity component at the edge of inner region II as $X \rightarrow \infty$ approaches that in the outer region when $x \rightarrow 0$ and consequently we have

$$\bar{\Delta}_1(Gr) = Gr^{-1/10} \quad (27)$$

and

$$\frac{\partial \bar{\psi}_1}{\partial X}(\infty, y) = \bar{\alpha}_1 y^{-1/5} \quad (28)$$

in which

$$\bar{\alpha}_1 = \frac{4}{5} f_0(\infty) / \sin(2\pi/5).$$

The equation for $\bar{\psi}_1$ is obtained by inserting expansion (26) into equation (1) where $\Phi = 0$ and retaining the lowest-order terms. This equation may be integrated once with respect to X and the resulting arbitrary function of y determined by using the matching condition (28). It can then be shown that

$$\frac{\partial^3 \bar{\psi}_1}{\partial X^3} + \frac{\partial \bar{\psi}_1}{\partial X} \frac{\partial^2 \bar{\psi}_1}{\partial y \partial X} - \frac{\partial \bar{\psi}_1}{\partial y} \frac{\partial^2 \bar{\psi}_1}{\partial X^2} = -\frac{1}{5} \bar{\alpha}_1^2 y^{-7/5}. \quad (29)$$

In this equation we write

$$\left. \begin{aligned} \bar{\psi}_1 &= y^{2/5} \bar{f}_1(\eta) \\ \bar{\eta} &= X/y^{3/5} \end{aligned} \right\} \quad (30)$$

and the equation satisfied by \bar{f}_1 is

$$\bar{f}_1''' - \frac{2}{5} \bar{f}_1 \bar{f}_1'' + \frac{1}{5} (\bar{\alpha}_1^2 - \bar{f}_1'^2) = 0 \quad (31)$$

with the boundary conditions

$$\left. \begin{aligned} \bar{f}_1(0) &= \bar{f}_1'(0) = 0 \\ \bar{f}_1 &\sim \bar{\alpha}_1 \bar{\eta} + \bar{A}_1, \quad \bar{\eta} \text{ large} \end{aligned} \right\} \quad (32)$$

where \bar{A}_1 is an unknown constant. Here the primes now signify differentiation with respect to $\bar{\eta}$.

It should be noted that with regard to the y -direction all the flow variables decay algebraically when $\bar{\eta}$ is large [33], whereas changes with respect to the x -direction are exponentially small when η tends to infinity. Further a generic streamline originates in the boundary-layer region II following a line $x = \text{const. } y^{2/5}$ at infinity. Then it crosses the outer edge of the boundary layer and enters the outer region along a line $x = \text{const. } y^{1/5}$.

3.5. Third-order flow in region III

Turning now to the outer region and using again the matching procedure that outer expansion (7) matches inner expansions (11) and (26) in the overlapping domain, where these expansions are valid, gives

$$\delta_2(Gr) = Gr^{-1/10} \quad (33)$$

and

$$\left. \begin{aligned} \tilde{\psi}_2(r, 0) &= 0 \\ \tilde{\psi}_2(r, \pi/2) &= \bar{A}_1 r^{2/5} \end{aligned} \right\} \quad (34)$$

Solving equation (10) for $\tilde{\psi}_2$ with boundary conditions (34) we obtain

$$\tilde{\psi}_2 = \bar{A}_1 r^{2/5} \sin(2\theta/5) / \sin(\pi/5). \quad (35)$$

This equation shows that the third-order outer streamlines enter boundary layer I at an angle $\pi/5$ to the x -axis.

3.6. Third-order boundary layer in region I

A further correction is needed in the inner flow region I to take care of the modification of the velocity at its boundary owing to the second-order outer flow. In this respect the matching condition yields

$$\Delta_2(Gr) = Gr^{-3/10} \quad (36)$$

and

$$\frac{\partial \psi_2}{\partial Y}(x, \infty) = \frac{2}{5} \bar{A}_1 x^{-3/5} / \sin(\pi/5). \quad (37)$$

On substitution of expansions (11) and (12) into equations (1) and (2) and collecting terms of equal order in $Gr^{-1/10}$ gives the equations satisfied by ψ_2 and Φ_2 . The introduction of the similarity variables

$$\psi_2 = x^{-2/5} f_2(\eta), \quad \Phi_2 = x^{-1} h_2(\eta) \quad (38)$$

reduces the third-order problem for inner layer I to

$$f_2''' + \frac{4}{5} f_0 f_2'' - \frac{2}{5} f_0' f_2 + h_2 = 0 \quad (39)$$

$$\sigma^{-1} h_2'' + \frac{4}{5} f_0 h_2' + f_0' h_2 = \frac{1}{5} h_0 f_2' + \frac{2}{5} f_2 h_0' \quad (40)$$

along with the boundary conditions

$$\left. \begin{aligned} f_2(0) = f_2'(0) = h_2'(0) = h_2(\infty) = 0 \\ f_2 \sim (\frac{2}{5}\bar{A}_1/\sin(\pi/5))\eta + A_2, \quad \eta \text{ large} \end{aligned} \right\} \quad (41)$$

where A_2 is an unknown constant.

3.7. Third-order boundary layer in region II

The matching condition of the third-order inner and outer velocities in the horizontal direction leads to

$$\bar{\Delta}_2(Gr) = Gr^{-1/5} \quad (42)$$

and

$$\frac{\partial \bar{\psi}_2}{\partial X}(\infty, y) = \bar{\alpha}_2 y^{-3/5} \quad (43)$$

where $\bar{\alpha}_2 = -\frac{2}{5}\bar{A}_1 \cot(\pi/5)$. The third-order term in inner expansion (26) of region II can now be determined from the third-order equation

$$\begin{aligned} \frac{\partial^3 \bar{\psi}_2}{\partial X^3} + \frac{\partial \bar{\psi}_1}{\partial X} \frac{\partial^2 \bar{\psi}_2}{\partial y \partial X} - \frac{\partial \bar{\psi}_1}{\partial y} \frac{\partial^2 \bar{\psi}_2}{\partial X^2} + \frac{\partial \bar{\psi}_2}{\partial X} \frac{\partial^2 \bar{\psi}_1}{\partial y \partial X} \\ - \frac{\partial \bar{\psi}_2}{\partial y} \frac{\partial^2 \bar{\psi}_1}{\partial X^2} = -\frac{4}{3}\bar{\alpha}_1 \bar{\alpha}_2 y^{-9/5} \end{aligned} \quad (44)$$

on using conditions (28) and (43). The solution of equation (44) may be written as

$$\bar{\psi}_2 = \bar{f}_2(\bar{\eta}) \quad (45)$$

where \bar{f}_2 is given by

$$\bar{f}_2''' - \frac{2}{3}\bar{f}_1 \bar{f}_2'' + \frac{4}{3}(\bar{\alpha}_1 \bar{\alpha}_2 - \bar{f}_1' \bar{f}_2') = 0 \quad (46)$$

with boundary conditions

$$\left. \begin{aligned} \bar{f}_2(0) = \bar{f}_2'(0) = 0 \\ \bar{f}_2 \sim \bar{\alpha}_2 \bar{\eta} + \bar{A}_2, \quad \eta \text{ large} \end{aligned} \right\} \quad (47)$$

where \bar{A}_2 is an unknown constant.

3.8. Fourth-order outer flow in region III

The fourth-order inner and outer terms may be treated in a similar manner to those already described. However, some extra care is required since the inner equations involve non-zero normal velocities across the free stream. Continuing the matching technique of the inner and outer stream functions implies that

$$\delta_3(Gr) = Gr^{-1/5} \quad (48)$$

and

$$\left. \begin{aligned} \bar{\psi}_3(r, 0) = A_1 \\ \bar{\psi}_3(r, \pi/2) = \bar{A}_2 \end{aligned} \right\} \quad (49)$$

The solution of equation (10) for $\bar{\psi}_3$ which satisfies conditions (49) is given by

$$\bar{\psi}_3 = \frac{2}{\pi}[\bar{A}_2 - A_1]\theta + A_1. \quad (50)$$

3.9. Fourth-order boundary layer in region I

Again, the matching procedure gives

$$\Delta_3(Gr) = Gr^{-2/5} \quad (51)$$

and

$$\frac{\partial \psi_3}{\partial Y}(x, \eta) \sim \left[\frac{2}{\pi}(\bar{A}_2 - A_1) + \frac{4}{25}\eta f_0(\infty) \right] x^{-1}, \quad \eta \text{ large.} \quad (52)$$

Setting the similarity solution

$$\psi_3 = x^{-4/5} f_3(\eta), \quad \Phi_3 = x^{-7/5} h_3(\eta) \quad (53)$$

and referring to the findings of the preceding sections, we obtain the following differential equations for f_3 and h_3 :

$$\begin{aligned} f_3''' + \frac{4}{3}f_0 f_3'' + \frac{2}{3}f_0' f_3 - \frac{4}{3}f_0'' f_3 + h_3 \\ = \frac{1}{25}(6f_0' - \eta^2 f_0''') - \frac{1}{3}f_1'^2 - \frac{1}{5}(2P + \eta P') \\ P' = \frac{1}{5}\eta f_0''' - \frac{2}{3}f_0'' + \frac{4}{25}\eta f_0' f_0'' \\ + \frac{1}{25}\eta f_0'^2 - \frac{16}{25}f_0 f_0' \end{aligned} \quad (54)$$

$$\begin{aligned} \sigma^{-1} h_3'' + \frac{4}{3}f_0 h_3' + \frac{2}{3}f_0' h_3 \\ = \frac{1}{3}h_0 f_3' + \frac{4}{3}h_0' f_3 - \frac{2}{3}h_1 f_1' \\ + \frac{1}{25}\sigma^{-1}(4h_0 - 4\eta h_0' - \eta^2 h_0'') \end{aligned}$$

with boundary conditions

$$\left. \begin{aligned} f_3(0) = f_3'(0) = h_3'(0) = h_3(\infty) = 0 \\ f_3 \sim \frac{2}{25}f_0(\infty)\eta^2 + \frac{2}{\pi}(\bar{A}_2 - A_1)\eta + A_3, \quad \eta \text{ large} \\ P \sim -\frac{8}{25}f_0^2(\infty)/\sin^2(2\pi/5), \quad \eta \text{ large.} \end{aligned} \right\} \quad (55)$$

Here P is called the pressure function and it is introduced in order to eliminate the pressure from the full Navier-Stokes equation.

3.10. Fourth-order boundary layer in region II

As before, if y is held fixed and X is allowed to be large, we find that

$$\bar{\Delta}_3(Gr) = Gr^{-3/10} \quad (56)$$

and

$$\frac{\partial \bar{\psi}_3}{\partial X}(\bar{\eta}, y) \sim \bar{\alpha}_3 y^{-1} \quad \text{for } \bar{\eta} \text{ large} \quad (57)$$

where

$$\begin{aligned} \bar{\alpha}_3 = -\frac{1}{125}f_0(\infty)\eta^2/\sin(2\pi/5) + \frac{6}{25}\bar{A}_1\bar{\eta} \\ - \frac{2}{\pi}(\bar{A}_2 - A_1). \end{aligned} \quad (58)$$

Now, if we let

$$\bar{\psi}_3 = y^{-2/5} \bar{f}_3(\bar{\eta}) \quad (59)$$

the following equation ensues for \bar{f}_3 :

$$\bar{f}_3''' - \frac{2}{3} \bar{f}_1 \bar{f}_3'' - \frac{9}{5} \bar{f}_1' \bar{f}_3' + \frac{2}{5} \bar{f}_1'' \bar{f}_3 = \frac{3}{5} \bar{f}_2'^2 + \frac{3}{5} (2\bar{P} + \bar{\eta} \bar{P}') - \frac{1}{25} (6\bar{f}_1' + 30\bar{\eta} \bar{f}_1'' + 9\bar{\eta}^2 \bar{f}_1''') \quad (60)$$

$$\bar{P}' = \frac{6}{25} \bar{\eta} \bar{f}_1 \bar{f}_1'' - \frac{4}{25} \bar{f}_1 \bar{f}_1' - \frac{3}{5} \bar{\eta} \bar{f}_1''' - \frac{4}{5} \bar{f}_1'' + \frac{9}{25} \bar{\eta} \bar{f}_1'^2 \quad (61)$$

with boundary conditions

$$\left. \begin{aligned} \bar{f}_3(0) &= \bar{f}_3'(0) = 0 \\ \bar{f}_3' &\sim \bar{\alpha}_3, \bar{\eta} \text{ large} \\ \bar{P} &\sim \frac{8}{125} f_0^2(\infty) \bar{\eta}^2 / \sin^2(2\pi/5) \\ &\quad - \frac{16}{125} f_0(\infty) \bar{A}_1 \bar{\eta} / \sin(2\pi/5) \\ &\quad - \frac{2}{25} \frac{\bar{A}_1^2}{\sin^2(\pi/5)} \\ &\quad + \frac{8}{5\pi} A_0(\bar{A}_2 - A_1) / \sin(2\pi/5), \bar{\eta} \text{ large.} \end{aligned} \right\} \quad (62)$$

4. EIGENSOLUTIONS

As in other related studies of higher-order boundary-layer approximations we now investigate the possibility on the existence of eigensolutions. We therefore add

$$\left. \begin{aligned} \psi^{(k)} &= C_k Gr^{-(1+\lambda_k)/5} x^{4(1-\lambda_k)/5} F_k(\eta) \\ \Phi^{(k)} &= C_k Gr^{-(1+\lambda_k)/5} x^{(1-4\lambda_k)/5} H_k(\eta) \end{aligned} \right\} \quad (63)$$

into the inner boundary-layer expansions (11) and (12) and

$$\bar{\psi}^{(k)} = \bar{C}_k Gr^{-(3+\lambda_k)/10} y^{2(1-\lambda_k)/5} \bar{F}_k(\bar{\eta}) \quad (64)$$

to the inner boundary-layer expansion (26). Here λ_k and $\bar{\lambda}_k$ are the eigenvalues associated with the inner boundary layers I and II, respectively, while C_k and \bar{C}_k are multiplicative constants being indeterminate, in general. The differential equations for the functions F_k and H_k coincide with those determined in refs. [10, 11] and are therefore not reproduced here. It was found that the first value of λ_k is $\lambda_1 = 5/4$ and all other values are greater than 2. Moreover, Mahajan and Gebhart [11] and Wilks [34] have demonstrated that the corresponding multiplicative constant to the first eigenvalue is identically zero, i.e. $C_1 = 0$.

The equation satisfied by \bar{F}_k is

$$\bar{F}_k''' - \frac{2}{3} \bar{f}_1 \bar{F}_k'' - \frac{2}{3} (1 + \bar{\lambda}_k) \bar{f}_1' \bar{F}_k' - \frac{2}{3} (1 - \bar{\lambda}_k) \bar{f}_1'' \bar{F}_k = 0 \quad (65)$$

and the boundary conditions are

$$\bar{F}_k(0) = \bar{F}_k'(0) = \bar{F}_k'(\infty) = 0. \quad (66)$$

A numerical inspection of these equations shows that they do not possess a solution for any real $\bar{\lambda}_k > 0$. Accordingly, expansions (11), (12) and (26) are correct to $O(Gr^{-3/5})$ and $O(Gr^{-1/2})$, respectively.

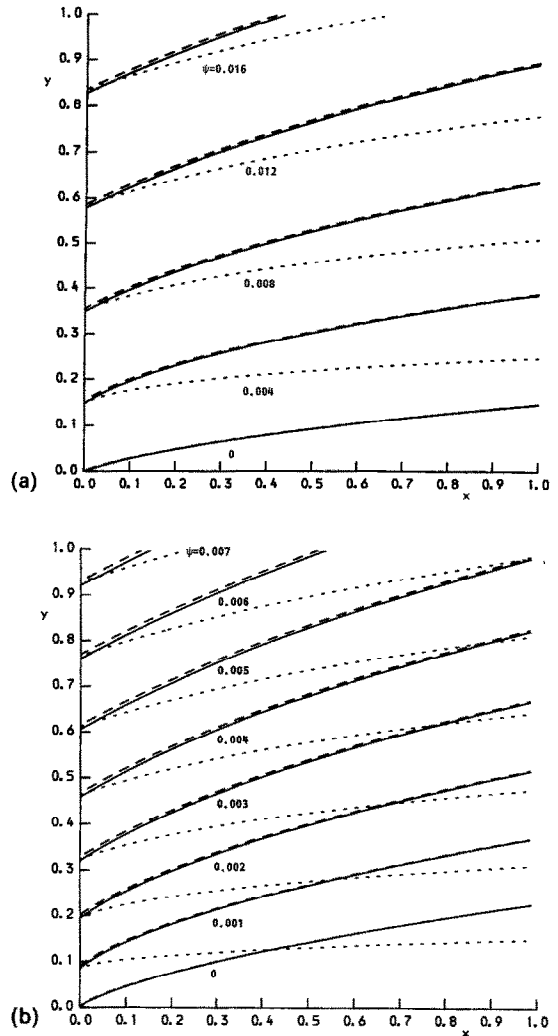


FIG. 2. The streamlines associated with the outer flow at $Gr = 10^{10}$ for (a) $\sigma = 0.72$, (b) $\sigma = 6.7$. -----, one term; -----, two terms; -----, three terms.

5. RESULTS AND DISCUSSION

The numerical results of the first-order perturbation functions f_0 and h_0 have been obtained in ref. [10] for the Prandtl numbers σ ranging from 0.03 to 10 and in ref. [11] for $\sigma = 0.733$ and 5.4. In this paper we have obtained the numerical values of the higher order perturbation functions (f_i, \bar{f}_i and $h_i, \bar{h}_i, i = 1, 2, 3$) associated with the inner stream functions and temperature for $\sigma = 0.72$ (air), 1 and 6.7 (water).

The fluid flow pattern outside the boundary layer is shown in Fig. 2 for $\sigma = 0.72$ and 6.7 with $Gr = 10^{10}$. Although these figures are similar it is seen, as expected, that the lower the Prandtl number the larger is the induced velocity in this region. The effects of the horizontal wall is to make the streamlines enter the vertical boundary layer such that they are convex upwards whereas in the absence of this wall the streamlines enter convex downwards. Similar flow patterns exist for other Grashof numbers but it is seen that even for $Gr = 10^{10}$ first-order corrections are

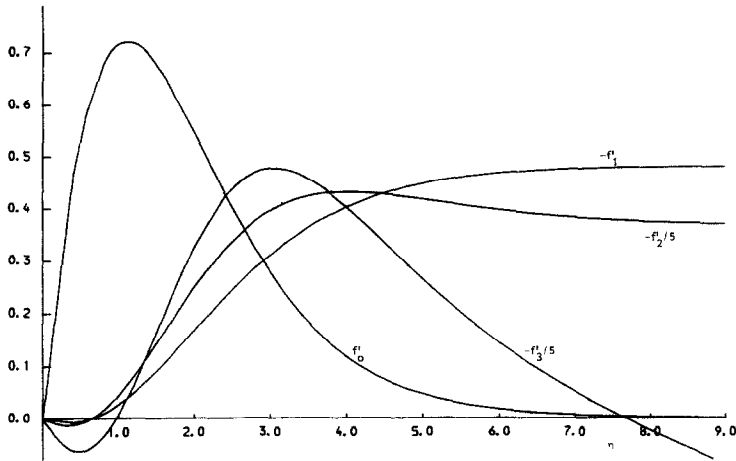


FIG. 3. The velocity function distribution on the vertical plate for $\sigma = 0.72$.

substantially affecting the flow. Therefore, the leading order solution is only appropriate at extremely large Grashof numbers.

The velocity near the vertical plate, the horizontal plate and temperature distribution, are given by

$$\left. \begin{aligned} \hat{u}\hat{x}\varepsilon_x/\nu &= f_0'(\eta) + \varepsilon_x f_1'(\eta) \\ &+ \varepsilon_x^{3/2} f_2'(\eta) + \varepsilon_x^2 f_3'(\eta) + \text{h.o.t.} \\ -\hat{v}\hat{y}\varepsilon_y/\nu &= \tilde{f}_1(\tilde{\eta}) + \varepsilon_y^{1/2} \tilde{f}_2(\tilde{\eta}) \\ &+ \varepsilon_y \tilde{f}_3(\tilde{\eta}) + \text{h.o.t.} \end{aligned} \right\}$$
$$\left. \begin{aligned} (T - T_0)k/(q\hat{x}\varepsilon_x) &= h_0(\eta) \\ &+ \varepsilon_x h_1(\eta) + \varepsilon_x^{3/2} h_2(\eta) \\ &+ \varepsilon_x^2 h_3(\eta) + \text{h.o.t.} \end{aligned} \right\}$$

(67)

and

respectively. Here ε_x and ε_y are the small parameters $\varepsilon_x = Gr_x^{-1/5}$ and $\varepsilon_y = Gr_y^{-1/5}$ with $Gr_x = g\beta q\hat{x}^4/(kv^2)$ and $Gr_y = g\beta q\hat{y}^4/(kv^2)$ denoting the Grashof numbers relative to the lengths \hat{x} and \hat{y} , respectively. The velocity and temperature profiles associated with expressions (67), i.e. the functions f_i' ($i = 0, 1, 2, 3$), h ,

($i = 0, 1, 2, 3$) and \tilde{f}_i' ($i = 1, 2, 3$) are plotted in Figs. 3–8.

It is observed that neglecting the second-order boundary-layer solution on the vertical plate will result in (i) an overestimation of the fluid velocity in the boundary layer except very close to the wall for the Prandtl number of 0.72 and (ii) an underestimation of the temperature profile in the boundary layer.

Having determined the velocity components and temperature fields we can evaluate the local Nusselt number and the skin friction coefficients at the plate as

$$Nu_x = \frac{\hat{x}q}{k(T_w - T_0)}$$

(68)

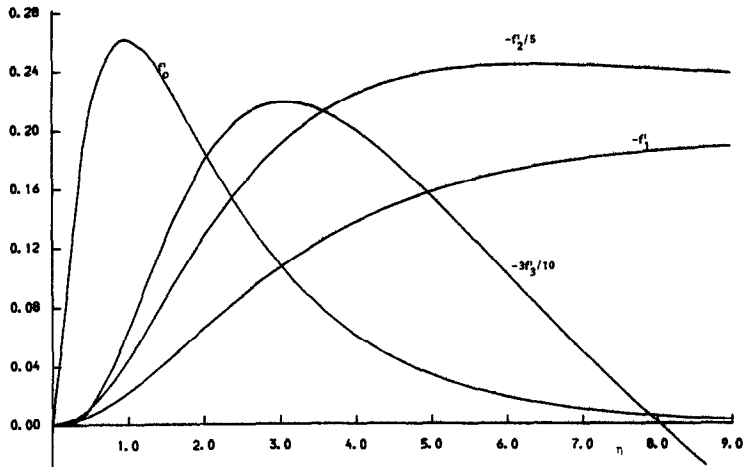
and

$$C_f^I = (L^2/\rho v^2) \left(\frac{\partial \hat{u}}{\partial \hat{y}} \right)_{\hat{y}=0},$$
$$C_f^{II} = (L^2/\rho v^2) \left(\frac{\partial \hat{v}}{\partial \hat{x}} \right)_{\hat{x}=0}.$$

(69)

FIG. 4. The temperature function distribution on the vertical plate for $\sigma = 0.72$.

FIG. 5. The velocity function distribution on the horizontal plate for $\sigma = 0.72$.


 FIG. 6. The velocity function distribution on the vertical plate for $\sigma = 6.7$.

After a little algebra, we obtain

$$\frac{Nu_x}{Nu_{x0}} = 1 - \epsilon_x \frac{h_1(0)}{h_0(0)} - \epsilon_x^{3/2} \frac{h_2(0)}{h_0(0)} - \epsilon_x^2 \left(\frac{h_3(0)}{h_0(0)} - \frac{h_1^2(0)}{h_0^2(0)} \right) - \dots \quad (70)$$

$$\left. \begin{aligned} &= 1 - 0.0803\epsilon_x - 0.6640\epsilon_x^{3/2} \\ &\quad - 1.4257\epsilon_x^2 + \dots, \quad \sigma = 0.72 \\ &= 1 - 0.0684\epsilon_x - 0.5754\epsilon_x^{3/2} \\ &\quad - 1.2164\epsilon_x^2 + \dots, \quad \sigma = 1.0 \\ &= 1 - 0.0320\epsilon_x - 0.3913\epsilon_x^{3/2} \\ &\quad - 0.6017\epsilon_x^2 + \dots, \quad \sigma = 6.7 \end{aligned} \right\} \quad (71)$$

and

$$\frac{C_f^I}{C_{f0}^I} = 1 + \epsilon_x \frac{f_1''(0)}{f_0''(0)} + \epsilon_x^{3/2} \frac{f_2''(0)}{f_0''(0)} + \epsilon_x^2 \frac{f_3''(0)}{f_0''(0)} + \dots \quad (72)$$

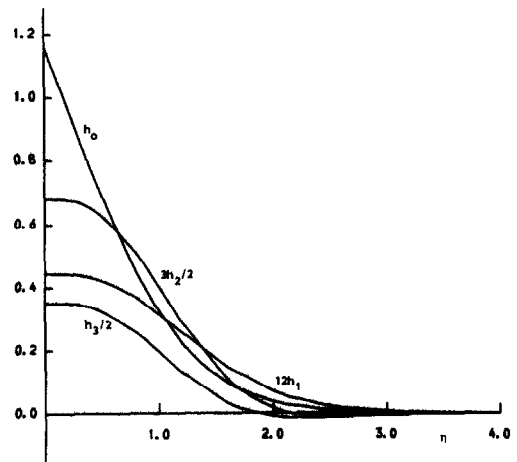
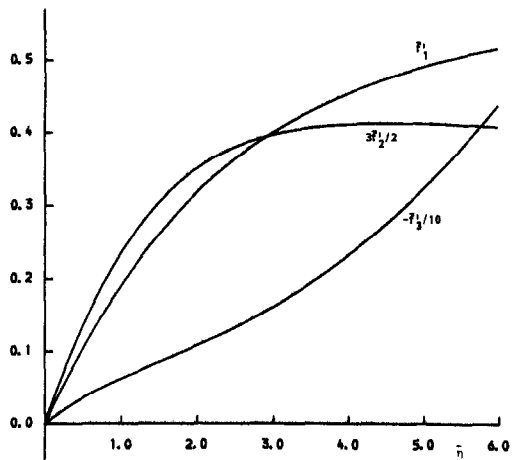
$$\left. \begin{aligned} &= 1 + 0.0344\epsilon_x - 0.2793\epsilon_x^{3/2} \\ &\quad + 0.8906\epsilon_x^2 + \dots, \quad \sigma = 0.72 \\ &= 1 + 0.0227\epsilon_x + 0.2023\epsilon_x^{3/2} \\ &\quad + 0.6762\epsilon_x^2 + \dots, \quad \sigma = 1.0 \\ &= 1 - 0.00612\epsilon_x + 0.01182\epsilon_x^{3/2} \\ &\quad + 0.0765\epsilon_x^2 + \dots, \quad \sigma = 6.7 \end{aligned} \right\} \quad (73)$$

$$\frac{C_f^{II}}{C_{f0}^{II}} = 1 + \epsilon_y^{1/2} \frac{\tilde{f}_2''(0)}{\tilde{f}_1''(0)} + \epsilon_y \frac{\tilde{f}_3''(0)}{\tilde{f}_1''(0)} + \dots \quad (74)$$

$$\left. \begin{aligned} &= 1 + 0.5873\epsilon_y^{1/2} - 2.3070\epsilon_y + \dots, \quad \sigma = 0.72 \\ &= 1 + 0.6072\epsilon_y^{1/2} - 2.6605\epsilon_y + \dots, \quad \sigma = 1.0 \\ &= 1 + 0.9152\epsilon_y^{1/2} - 3.7832\epsilon_y + \dots, \quad \sigma = 6.7 \end{aligned} \right\} \quad (75)$$

where the suffix '0' refers to the zeroth-order boundary-layer results.

From expression (71) it is seen that the zero-order boundary layer underpredicts the local Nusselt num-


 FIG. 7. The temperature function distribution on the vertical plate for $\sigma = 6.7$.

 FIG. 8. The velocity function distribution on the horizontal plate for $\sigma = 6.7$.

ber at all orders of the approximations made and Prandtl numbers considered. This is in direct contrast to the situation that occurs without the presence of the horizontal plate, see Mahajan and Gebhart [11]. However, this result is not unexpected because the presence of the horizontal plate has a profound effect on the induced flow away from the solid boundaries as we observed earlier.

The effects of the higher-order approximations on the skin friction coefficient on the vertical plate, see equation (73), are observed to be dependent on the value of the Prandtl number. On further investigation it is found that if $\sigma \lesssim (\gtrsim) 3.055$ the first-order boundary-layer correction underestimates (overestimates) the zero-order boundary-layer solution. It should be noted that in the absence of the horizontal plate Mahajan and Gebhart [11] solved this problem but there is a sign error in their Table 1 in which $f''(0)$ should take the positive value 0.006691. If this correction is made then their results again give the opposite tendencies to those of the present work for the reasons already given.

The leading order correction to the boundary-layer solution on the horizontal wall increases the skin friction whilst the next order correction decreases it for all the Prandtl numbers we considered.

In conclusion it is observed that even at local Grashof numbers of $O(10^{10})$ higher-order approximations are beginning to have an appreciable effect on the flow characteristics and hence the classical boundary-layer solution may only be used with confidence at extremely large Grashof numbers. Further the leading order correction term to the vertical boundary-layer solution has precisely the opposite effect to that observed without the presence of the horizontal boundary. In order to obtain higher-order corrections it has been shown that it is necessary to include the interaction between the two boundary-layer flows which takes place by inertia effects through the outer region, which is both inviscid and isothermal.

Acknowledgement—The helpful comments of the referees were very much appreciated.

REFERENCES

1. K.-T. Yang and E. W. Jerger, First order perturbations of laminar free convection boundary layers on a vertical plate, *J. Heat Transfer* **86**, 107–115 (1964).
2. W. T. Kierkus, An analysis of laminar free convection flow and heat transfer about an inclined isothermal plate, *Int. J. Heat Mass Transfer* **11**, 241–253 (1968).
3. V. Kadambi, Singular perturbations in free convection, *Wärme- und Stoffübertr.* **2**, 99–104 (1969).
4. C. A. Hieber, Natural convection around a semi-infinite vertical plate: higher order effects, *Int. J. Heat Mass Transfer* **17**, 785–791 (1974).
5. N. Riley, Note on a paper by Kierkus, *Int. J. Heat Mass Transfer* **18**, 991–993 (1975).
6. D. S. Riley and D. G. Drake, Higher approximations to the free convection flow from a heated vertical flat plate, *Appl. Scient. Res.* **30**, 193–207 (1975).
7. A. F. Messiter and A. Liñán, A vertical plate in a laminar free convection: effects of leading and trailing edges and discontinuous temperature, *ZAMP* **27**, 633–651 (1976).
8. A. A. Berezovsky, O. G. Martynenko and Yu. A. Sokovishin, Free convection heat transfer on a vertical semi-infinite plate, *J. Engng Phys.* **33**, 32–39 (1977).
9. A. A. Berezovsky and Yu. A. Sokovishin, The leading edge effects on free-convective heat transfer, *J. Engng Phys.* **33**, 501–504 (1977).
10. A. A. Berezovsky and Yu. A. Sokovishin, The singular perturbation method in the problem of free convection with a constant heat flux on a vertical surface, *Izv. Akad. Nauk SSR, Mekh. Zhid. Gaza* No. 2, 129–136 (1977).
11. R. L. Mahajan and B. Gebhart, Higher order approximations on the natural convection flow over a uniform flux vertical surface, *Int. J. Heat Mass Transfer* **21**, 549–556 (1978).
12. R. L. Mahajan and B. Gebhart, Higher-order boundary layer effects in plane horizontal natural convection flows, *J. Heat Transfer* **102**, 368–371 (1980).
13. O. G. Martynenko, A. A. Berezovsky and Yu. A. Sokovishin, Laminar free convection from a vertical plate, *Int. J. Heat Mass Transfer* **27**, 869–881 (1984).
14. N. Afzal, Higher order effects in natural convection flow over a uniform flux horizontal surface, *Wärme- und Stoffübertr.* **19**, 177–180 (1985).
15. N. Riley, Free convection from a horizontal line source of heat, *ZAMP* **25**, 817–828 (1974).
16. C. A. Hieber and E. J. Nash, Natural convection about a line heat source: higher order effects and stability, *Int. J. Heat Mass Transfer* **18**, 1473–1479 (1975).
17. N. Afzal, Convective wall plume: higher order analysis, *Int. J. Heat Mass Transfer* **23**, 504–513 (1980).
18. R. Krishnamurthy and B. Gebhart, Mixed convection in wall plumes, *Int. J. Heat Mass Transfer* **27**, 1679–1689 (1984).
19. R. Krishnamurthy and B. Gebhart, Mixed convection from a line source plume, *Int. J. Heat Mass Transfer* **29**, 344–347 (1986).
20. I. C. Walton, Second order effects in free convection, *J. Fluid Mech.* **64**, 796–809 (1974).
21. K. Gersten and J. S. d'Avila, Higher order boundary layer effects in combined free and forced convection, European Space Agency (ESA-TT-498), pp. 122–131 (1979).
22. P. Cheng, Natural convection in a porous medium: external flow. In *Natural Convection: Fundamentals and Applications* (Edited by S. Kakac et al.). Hemisphere, Washington, DC (1985).
23. D. A. Nield, Recent research on convection in a porous medium. In *Proc. CSIRO/DSIR Seminar on Convective Flows in Porous Media*, Wellington, New Zealand (1985).
24. M. Van Dyke, *Perturbation Methods in Fluid Mechanics*. Academic Press, New York (1964).
25. O. G. Martynenko, A. A. Berezovsky and Yu. A. Sokovishin, *The Asymptotic Methods in the Free-convection Heat Transfer Theory* (in Russian). Izd. Nauki i Tekhnika, Minsk (1979).
26. D. S. Riley and G. Poorts, Thermal convection in a heated vertical corner, *Q. J. Mech. Appl. Math.* **25**, 401–421 (1972).
27. C. Rodighiero and L. M. de Socio, Some aspects of natural convection in a corner, *J. Heat Transfer* **105**, 212 (1983).
28. P. Luchini, A. Pozzi and L. M. de Socio, Convezione naturale in un angolo. In *Atti 37° Congresso Nazionale ATI*, Padova, pp. 615–622, Sept. (1982).
29. P. Luchini, Analytical and numerical solutions for natural convection in a corner, *AIAA J.* **24**, 841–848 (1986).
30. R. Ruiz and E. M. Sparrow, Natural convection in V-shaped and L-shaped corners, *Int. J. Heat Mass Transfer* **30**, 2539–2548 (1987).
31. M. H. Kim and M.-U. Kim, Natural convection near a

- rectangular corner, *Int. J. Heat Mass Transfer* **31**, 1357–1364 (1988).
32. D. B. Ingham and I. Pop, A note on free convection flow in a corner, *Int. Commun. Heat Mass Transfer* **15**, 315–322 (1988).
33. L. Rosenhead (Editor), *Laminar Boundary Layers*, p. 247. Oxford University Press, London (1963).
34. G. Wilks, The flow of a uniform stream over a semi-infinite vertical flat plate with uniform surface heat flux, *Int. J. Heat Mass Transfer* **17**, 743–753 (1974).

CONVECTION NATURELLE DANS UN COIN A ANGLE DROIT: ANALYSE D'ORDRE ELEVE

Résumé—On présente des effets de couche limite d'ordre élevé pour la convection naturelle dans un coin à angle droit formé par une plaque verticale semi-infinie, à flux thermique constant, et une plaque horizontale semi-infinie isolée thermiquement. En utilisant la méthode de développement asymptotique la solution est obtenue jusqu'à l'ordre quatre. On étudie pour la première fois l'interaction des deux écoulements de couche limite à travers la région externe non visqueuse. On a considéré les valeurs propres et leurs fonctions propres associées aux développements internes et on a trouvé que leur contribution est identiquement nulle jusqu'à la correction d'ordre quatre. Des résultats numériques sont obtenus pour des nombres de Prandtl de 0,72 (air), 1 et 6,7 (eau) et on présente l'écoulement dans la région externe ainsi que les profils de vitesse et de température dans les couches limites. La variation du nombre de Nusselt local et des coefficients de frottement pariétal est présentée en fonction du nombre de Grashof local. On trouve que la présence du plan horizontal a un effet très marqué sur les approximations d'ordre élevé dans la couche limite verticale et dans la région externe.

NATÜRLICHE KONVEKTION IN EINER RECHTWINKLIGEN ECKE: ANALYSE HÖHERER ORDNUNG

Zusammenfassung—In dieser Arbeit werden die Grenzschichteffekte höherer Ordnung für eine natürliche Konvektionsströmung in einer rechtwinkligen Ecke beschrieben. Diese Ecke wird von einer halbunendlichen vertikalen Platte, der ein einheitlicher Wärmestrom aufgeprägt ist, und einer halbunendlichen horizontalen Platte, die wärmegeklämt ist, gebildet. Unter Benutzung der Methode der asymptotischen angepassten Entwicklungen ergibt sich die Lösung bis zu einer Entwicklung der vierten Ordnung. Hier wurde zum ersten Mal das Zusammenspiel zwischen den beiden Grenzschichtströmungen untersucht, die durch die äußere reibungsfreie Region bedingt sind. Die Eigenwerte und ihre entsprechenden Eigenfunktionen, die über die innere Entwicklung zugeordnet sind, werden aufgesucht, und es ergibt sich, daß ihr Beitrag bis zu einer Korrektur vierter Ordnung genau null ist. Für Prandtl-Zahlen von 0,72 (Luft) sowie 1 und 6,7 (Wasser) erhält man numerische Lösungen, und es werden die Strömung in der äußeren Region sowie die Geschwindigkeits- und Temperaturprofile in den Grenzschichten dargestellt. Außerdem werden Variationen der lokalen Nusselt-Zahl und der Reibungsbeiwerte der Platten als Funktion der lokalen Grashof-Zahl aufgezeigt. Es ergibt sich, daß die Präsenz der horizontalen Platten einen sehr wesentlichen Effekt auf die Näherungslösungen höherer Ordnung in der vertikalen Grenzschicht und der äußeren Region hat.

ЕСТЕСТВЕННАЯ КОНВЕКЦИЯ ВБЛИЗИ ПРЯМОГО УГЛА: АНАЛИЗ ВЕЛИЧИН ВЫСШЕГО ПОРЯДКА

Аннотация—Исследуются эффекты высшего порядка в пограничных слоях при естественноконвективном течении вблизи прямого угла, образованного полубесконечными пластинами. Вертикальная пластина нагревается равномерно, горизонтальная—теплоизолирована. Методом сращиваемых асимптотических разложений получено решение до величин четвертого порядка. Впервые исследовано взаимодействие двух течений в пограничных слоях во внешней невязкой области. Найлены собственные значения и соответствующие им собственные функции разложения для внутренней области. Обнаружено, что их вклад в поправку четвертого порядка тождественно равен нулю. Получены численные результаты для числа Прандтля, равного 0,72 (воздух), 1 и 6,7 (вода) при течении во внешней области, и приведены профили температуры и скорости в пограничных слоях. Представлены также зависимости локального числа Нуссельта и коэффициента поверхностного трения на пластинах от числа Грасгофа. Показано, что горизонтальная пластина оказывает существенное влияние на приближения высшего порядка в вертикальном пограничном слое и во внешней области.